Reproducibility of pop-in using heterogeneous welded joint specimen and cohesive surface model

Sohei Kanna [1,1], *Yoichi* Yamashita [1] , and *Tomoya* Kawabata [2]

[1]Research Laboratory, IHI Corporation, Yokohama 235-8501, Japan
[2]Department of Systems Innovation, The University of Tokyo, Tokyo 113-8656, Japan

Abstract. When a pop-in as a phenomenon of initiation, propagation, and arrest of a brittle crack occurs in the fracture toughness test, the fracture toughness may be evaluated extremely low. In order to identify the cause of pop-in occurrence, an objective of this study was to demonstrate pop-ins in the three-point bend fracture toughness tests. It was possible to reproduce pop-ins at LBZ zone by preparing the specimens containing heterogeneous weld metals and considering the temperature dependency of the toughness in each welding material. Furthermore, the pop-in occurrence could be simulated by finite element analysis using a cohesive surface.

1 Introduction

In the three-point bend fracture toughness test on a welded joint, a small brittle crack may be formed at a tip of a fatigued pre-crack and arrest following slight propagation before attaining final rupture. The phenomenon is called a pop-in. The current Standards [1-5] including pop-ins assessment procedure can be too conservative in terms of judging their occurrence as catastrophic failure of welded structures [6]. Studies to investigate the pop-in phenomenon and to review allowable criteria of the current Standards are important for practical use in the manufacture and maintenance of the welded structures.

In this report, in order to examine future pop-in assessment against final catastrophic failure, a heterogeneous welded joint was produced and aimed to reproduce pop-in under three-point bending test conditions. In addition, a damage analysis was carried out to simulate the pop-in by finite element analysis using a cohesive surface.

2 Experiment

2.1 Condition

A brittle crack may be observed at the fatigue pre-crack tip of the specimen where pop-in occurred [7]. At this time, a local brittle zone (LBZ) may exist in a heat affected zone (HAZ) [8]. Heterogeneity is a feature of fracture of welded joints.

[1] Corresponding author: souhei_kanna@ihi.co.jp

In order to reproduce the pop-in, a heterogeneous material welded joint was made of a low toughness welded material at the center of the thickness and a high toughness welded material at both surrounding sides. Then, the joint was processed into three-point bending test specimens. Fig. 1 shows the dimensions of the heterogeneous welded joint and the three-point bending specimen. Table 1 shows the mechanical properties of base and weld materials, which were obtained from the round bar tensile tests using the specimens with its diameter of 3 mm.

The temperature of the round bar tensile tests was −80°C, which was the same temperature as the three-point bend fracture toughness tests. Here, Satoh et al. [9] measured the temperature dependence of the fracture toughness of 780 MPa class high-tensile-strength steel and the austenitic stainless steel SUS 304. Based on their measurement results, the temperature at which only the low toughness material fractured brittle was determined. It should be noted that austenitic stainless steel has excellent toughness even at cryogenic temperatures [10].

Fatigue cracks may not propagate on welded joint specimens due to compressive welding residual stress. Therefore, all specimens were subjected to local compression (platen) process at room temperature in order to equalize the pre-crack front edge shape. The platen process is the technique of pushing the notch of the specimen in the thickness direction and releasing the residual stress by plastic deformation [3].

After platen process, the room temperature fatigue tests were conducted. Here, the condition that does not exceed the load and the stress intensity factor of 30.9 MPa√m specified in WES 1108 [4] obtained from the critical crack tip opening displacement (CTOD) of 0.01 mm were set. The fatigue pre-cracks were propagated by 2 mm as average values of the front and back surfaces. Therefore, the ratio of the initial crack length of 30 mm to the width of 60 mm was about 0.5.

The load span of the three-point bending test was 240 mm which was 4 times the width according to WES 1108 [4]. The tests were carried out at the test temperature −80 °C with at a loading crosshead speed of 0.5 mm/min.

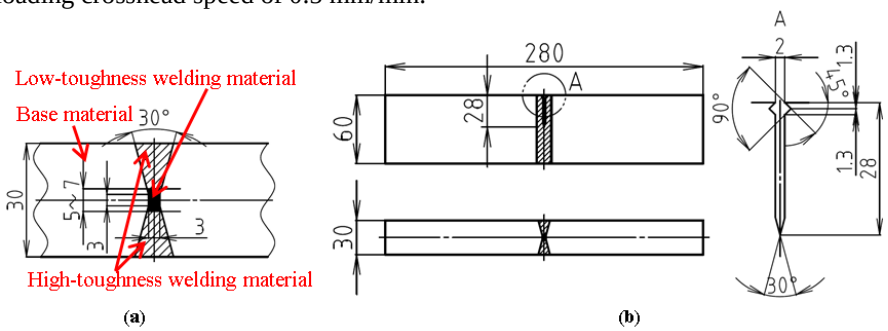

Fig. 1. Dimensions: (a) Heterogeneous weld joint. (b) three-point bending specimen. (unit: mm)

Table 1. Mechanical properties of yield strength, σ_Y, tensile strength, σ_T, elongation, A, reduction of area, Z and Young's modulus, E, of base and weld materials.

Material	Standard	σ_Y [MPa]	σ_T [MPa]	A [%]	Z [%]	E [MPa]
Base material	WEL-TEN 780E	750	890	16.2	70	198000
Welding material						
Low-toughness	AWS A5.5 E11016-G	940	1000	19.4	69	202900
High-toughness	AWS A5.4 E312-16	670	955	25.4	47	190600

2.2 Result

Two clip gauges were attached to the front and back sides of the notch mouse of the specimen respectively, so that a discontinuous changes in the load, P, - clip gauge opening displacement, V_g curves could be detected. Fig. 2 shows the P-V_g curves in the three-point bending test results. Here, V_g is the average value of two clip gauges. For all three specimens, the discontinuous changes occurred in the P-V_g curves during the tests. At this time, the tests were stopped and unloaded to confirm the pop-in cracks after fracture surface observations. The fatigue cracks propagated in the room temperature fatigue tests, and the specimens were fractured to observe. The "FEM" in Fig. 2 is described in the next chapter.

Fig. 3 shows the macro fractography of specimen No. 1, 2 and 3. The edges of the fatigue pre-cracks and the pop-in cracks are shown by dotted and broken lines in the lower part of Fig. 3. From Fig. 3, the pop-in cracks can be distinguished from the fatigue cracks before the three-point bending tests and the fatigue cracks fractured after the tests, because the appearance is clearly different.

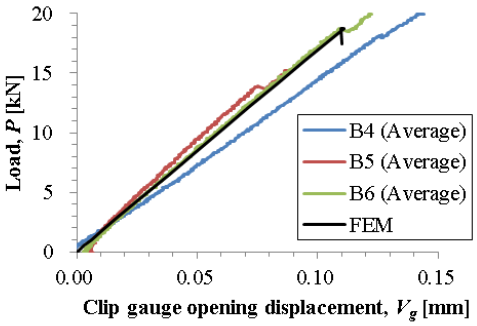

Fig. 2. Load-clip gauge opening displacement (average of front and back sides) curves.

3 Analysis

3.1 Condition

In order to simulate pop-in analytically, a damage analysis by finite element method (FEM) using a cohesive surface [11] was carried out. Geometric nonlinearity was considered for the analysis, and it was divided into Step 1 and Step 2 before and after the pop-in. Step 1 was an implicit static analysis and Step 2 was an explicit dynamic analysis. The general purpose software, Abaqus/Standard [12] and Abaqus/Explicit [13], were used, respectively.

The material constants were set by combining the round bar tensile test results and the fitted the Swift's equations [14]. The true stress, σ_t, - the true plastic strain, ε_p, curves input to the analysis is shown in Fig. 4. Poisson's ratio, ν, was set to 0.3 for all. The density was all set to 7.85×10^3 kg/m^3. Furthermore, considering the strain rate dependency in dynamic effect, it was defined by the power law of Cowper-Symonds [15] of the following equation.

$$\sigma_{x,\mathrm{dynamic}}\left(\epsilon_p, \dot{\epsilon}_p\right) = \sigma_{x,\mathrm{static}}\left(\epsilon_p\right) \cdot \left[1 + \left(\frac{\dot{\epsilon}_p}{C}\right)^{1/P}\right] \quad (1)$$

Based on the study of Kawabata et al. [16], C was set to 5.04×10^4 [1/s] and P to 5.14[-].

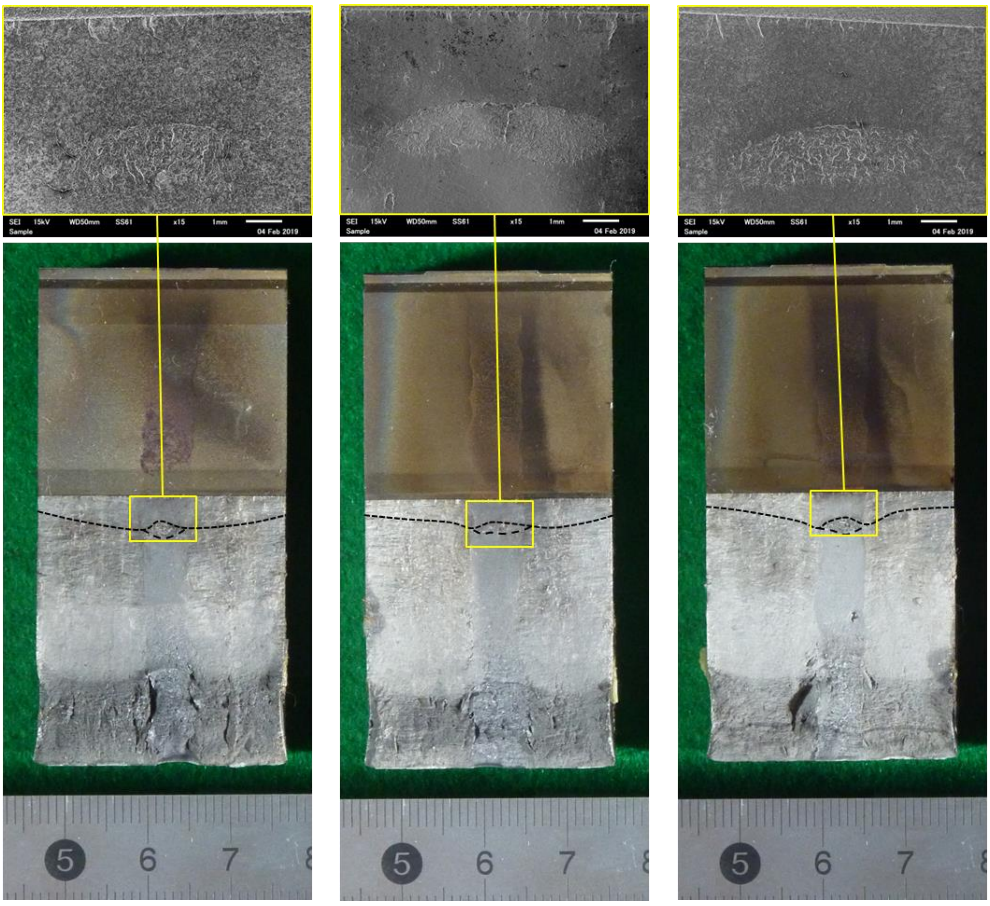

Fig. 3. Macro fractography: (a) No. 1. (b) No. 2. (b) No. 3

Fig. 5 shows the analytical model. The receiving jig located at the center of the specimen was modelled with an analytically rigid surface without friction, and the reference node was full constrained. The element used 8-node primary element. The finite elements meshes located in the crack propagation direction were sufficiently fine and the minimum element size was 0.1 mm.

In Step 1, the three-point bending test result of specimen No. 3, which has the P-V_g curve of Fig. 2 most similar to the analytical result, was taken as the analytical condition. The forced displacement to be applied to the analytical model was set to 0.193 mm so that the load 18.7 kN when pop-in occurred in No. 3 was matched.

On the center of the specimen which was specularly symmetrical, Y-Z symmetry condition was set in Step 1, and the damage law was set as cohesive surface in Step 2. However, one line of elements (0.1 mm) in contact with the receiving jig was set as contact surface so as not to be damaged by the jig. The crack opening stress contour in Step 1 is shown in Fig. 6. From Fig. 6, among the damage laws of low toughness materials, the peak stress at the position of r = 0.1 mm was adopted as the characteristic distance stress in the limit fracture stress in the tensile direction. It seemed that processes such as actual fracture continuation and regeneration often occurred at near points from the crack tip.

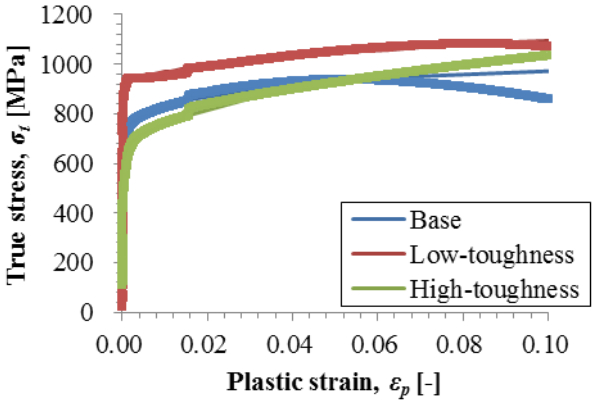

Fig. 4. Relationship between true stress and plastic strain. (Plot: Round bar tensile test results)

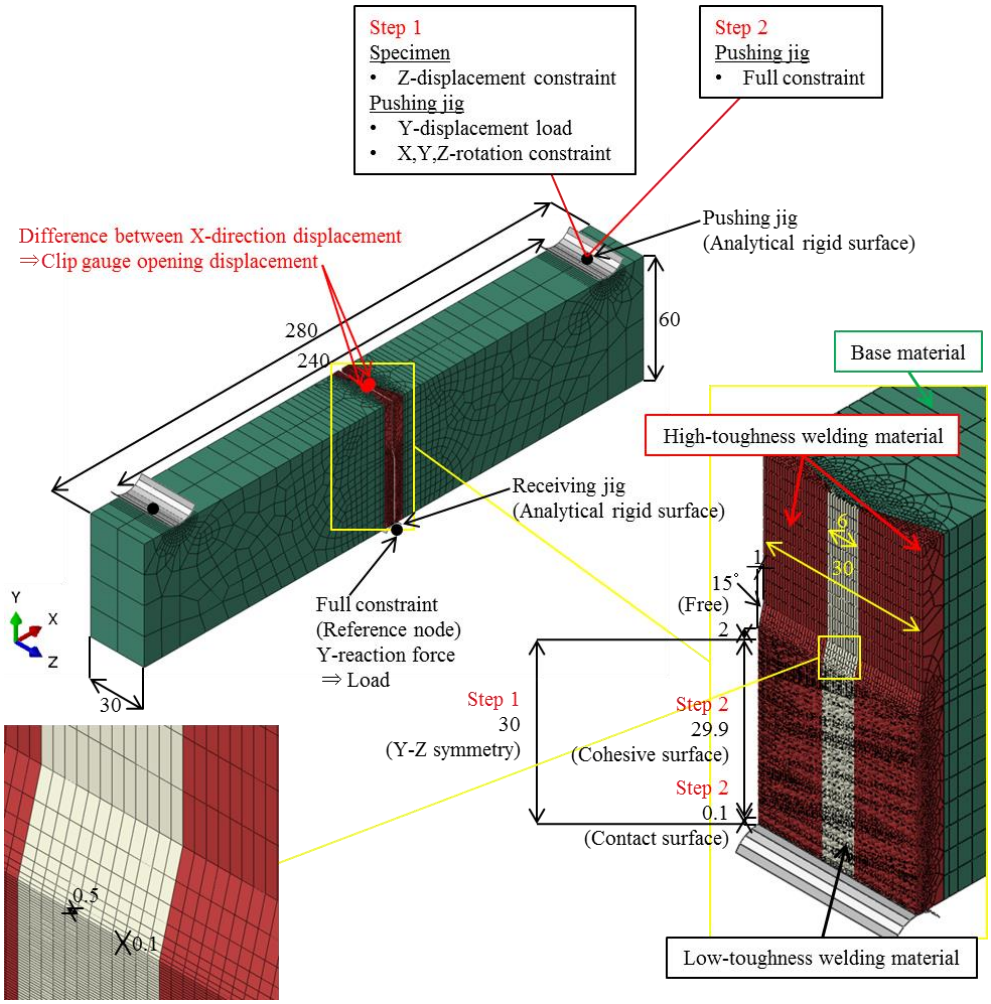

Fig. 5. Analytical model. (unit: mm)

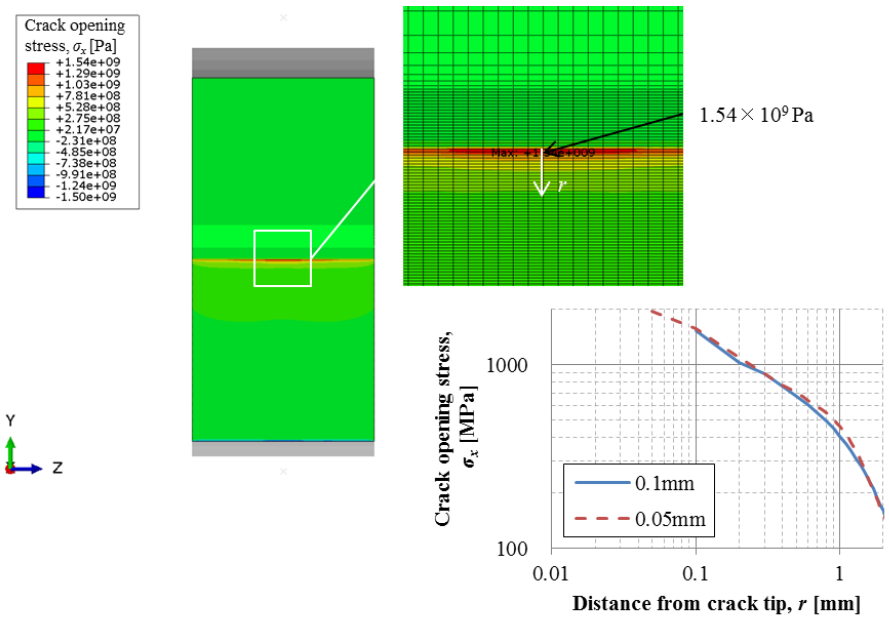

Fig. 6. Crack opening stress contour from analytical result in Step 1.

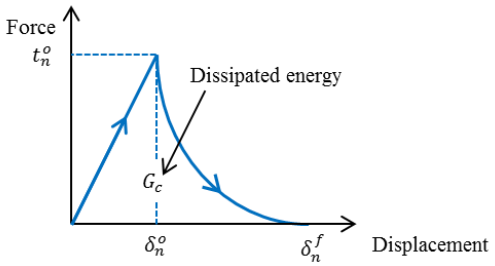

Fig. 7. Exponential damage development of cohesive surface

Table 2. Damage law of nominal stress, t_n^o, 1st and 2nd shear stress, t_s^o, t_t^o, and fracture energy, G_c of weld materials.

Material	Damage initiation		Damage development
	t_n^o [Pa]	t_s^o, t_t^o [Pa]	G_c [J/m^2]
Welding material			
Low-toughness	1.54×10^9	1.54×10^{11}	1.00×10^3
High-toughness	1.54×10^{11}	1.54×10^{13}	1.00×10^5

However, the stress distribution within the characteristic distance was considered to be almost the same if the characteristic distance stresses are equal, and the characteristic distance stress was adopted as the toughness. Furthermore, the same analysis was carried out in the model with minimum element size set to 0.05 mm, and it was confirmed that the stress distributions were almost identical as shown in Fig. 6. The limiting fracture stresses in the 1st and 2nd shear directions were 100 times the tensile direction. The damage was developed in the exponential form shown in Fig. 7. The fracture energy was adjusted so

that the brittle crack length became about 1.5 mm from Fig. 3(c). The damage law of the high toughness material was set to 100 times that of the low toughness material. Table 2 shows the damage law.

3.2 Result

The "FEM" in Fig. 2 shows the load, P, - clip gauge opening displacement, V_g, curve of the analytical result. P was the Y-direction reaction force of the full constrained reference node. Also, V_g was the difference between the X-direction displacement of two nodes at the center of the machine notch mouth. From Fig. 2, the P-V_g curves of "FEM" and "No. 3" were in good agreement.

Fig. 8 shows the damage variable contour from the analytical result in Step 2. In the region where the damage variable is 1.0, it indicates that the damage law are satisfied and the cohesive surface has separated [17]. As shown in Fig. 8, the length of the brittle crack was approximately 1.3 mm as set by the fracture energy of the appropriate damage law. Therefore, the three-point bending test result could be simulated.

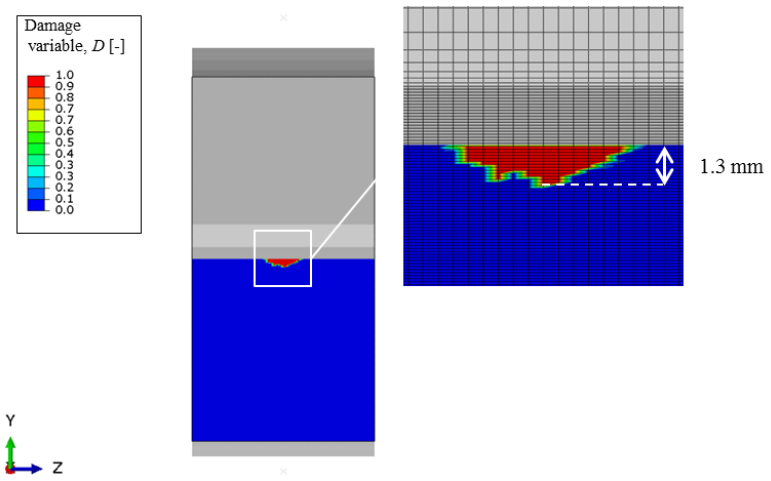

Fig. 8. Damage variable contour from analytical result in Step 2.

4 Conclusion

The welded joint containing heterogeneous weld metals was produced. Using the specimens cut from the joint, three-point bending tests were carried out at the temperature at which only the low toughness material fractured brittle. From the three-point bending test results, the discontinuous changes in the load-clip gauge opening displacement curves and the brittle cracks on the fracture surfaces were confirmed. Therefore, the pop-in was successfully reproduced.

Furthermore, by finite element analysis using the cohesive surface, the pop-in could be simulated by using the appropriate parameters.

The authors thank the members of the Commission CTE of the Japanese Welding Engineering Society for fruitful discussions that helped this study.

References

1. ASTM E399-17. Standard test method for linear-elastic plane-strain fracture toughness KIc of metallic materials, ASTM International (2017)

2. ISO 12135. Metallic materials—Unified method of test for the determination of quasistatic fracture toughness, International Organization for Standardization (2016)

3. ISO 15653. Metallic materials—method of test for the determination of quasistatic fracture toughness of welds, International Organization for Standardization (2018)

4. WES 1108. Standard test method for crack-tip opening displacement (CTOD) fracture toughness measurement, The Japan Welding Engineering Society (2016)

5. WES 1109. Guideline for crack-tip opening displacement (CTOD) fracture toughness test method of weld heat-affected zone, The Japan Welding Engineering Society (1995)

6. K. Arimochi, K. Isaka. A study on pop-in phenomenon in CTOD test for weldment and proposal of assessment method for significance of pop-in, IIW Doc. X-1118-86 (1986)

7. M.G. Dawes, H.G. Pisarski, S.J. Squirrel. Squirrel SJ. Fracture mechanics tests on welded joints, ASTM STP 995k, 191-213 (1989)

8. T. Haze, S. Aihara. Metallurgical factors controlling HAZ toughness in HT50 steels, IIW Doc. IX-1423-86 (1986)

9. K. Satoh, M. Toyoda, F. Minami. Effects of fracture controlling factors on cleavage fracture initiation in specimens with heterogeneity along crack front, Journal of the Japan Welding Society, **50**, 743-749 (1981) [in Japanese]

10. M.F. McGuire, *Encyclopedia of Materials: Science and Technology* (Elsevier Ltd, 2001)

11. G.T. Camacho, M. Ortiz. Computational modelling of impact damage in brittle materials, International Journal of Solids and Structures, **33**, 2899-2938 (1996)

12. Dassault Systems, Abaqus/Standard, version 6.14-1 (2014)

13. Dassault Systems, Abaqus/Explicit, version 6.14-1 (2014)

14. H.W. Swift. Plastic instability under plane stress, Journal of the Mechanics and Physics of Solids, **1**, 1-18 (1952)

15. G.R. Cowper, P.S. Symonds. Strain-hardening and strain-rate effects in the impact loading of cantilever beams, Brown University, Division of Applied Mathematics technical report, **28**, (1957)

16. T. Kawabata, A. Inami, S. Aihara. Numerical model of brittle crack propagation considering fracture surface energy on high tensile strength steel—Proposal of numerical model of brittle crack propagation (report 1) –, Journal of the Japan Society of Naval Architects and Ocean Engineers, **16**, 77-87 (2012), [in Japanese]

17. Dassault Systems, Abaqus Analysis User's guide (2015)